УДК 621.039.61

NUMERICAL STUDY OF FIRST ORBIT LOSSES OF TRAPPED PARTICLES IN TOKAMAKS

N.A. Azarenkov, Zh.S. Kononenko
V.N. Karazin Kharkiv National University
Svobody sq. 4, 61077, Kharkiv, Ukraine
e-mail: kononenko_zh@mail.ru
Received 30 April, 2009

The analytical model of the 2D tokamak magnetic field for the test particle simulations is proposed. It is shown how to vary the model parameters to obtain the plasma shape with the different ellipticity and triangularity. The problems of the particle direct losses in tokamak are discussed. The loss cones of the particles are calculated for the different initial radial locations. The minimum trapped particle energy required to escape from the plasma due to the first orbit losses is found numerically for the different ion species.
KEY WORDS: rotational transform, Poincare plot, trapped and passing particles, direct losses, loss cone.

ЧИСЛЕННОЕ ИЗУЧЕНИЕ ПРЯМЫХ ПОТЕРЬ ЗАПЕРТЫХ ЧАСТИЦ В ТОКАМАКАХ
Н.А. Азаренков, Ж.С. Кононенко
Харьковский национальный университет им. В.Н. Каразина,
пл. Свободы, 4, 61077, г. Харьков, Украина
Предложена аналитическая модель 2D магнитного поля токамаков для моделирования методом тестовых частиц. Показано, как посредством изменения модельных параметров добиться сечения плазмы с разным значением эллиптичности и треугольности. Проанализированы вопросы прямых потерь частиц в токамаках. Построены конусы потерь частиц для различных начальных радиальных положений. Численно найдена минимальная энергия, при которой возможна прямая потеря запертых частиц из плазмы, для различных сортов ионов плазмы.
КЛЮЧЕВЫЕ СЛОВА: угол вращательного преобразования, отображение Пуанкаре, запертые и пролетные частицы, прямые потери, конус потерь.

ЧИСЛОВЕ ДОСЛІДЖЕННЯ ПРЯМИХ ВТРАТ ЗАХОПЛЕНИХ ЧАСТИНОК У ТОКАМАКАХ
М.О. Азарєнков, Ж.С. Кононенко
Харківський національний університет ім. В.Н. Каразіна
пл. Свободи, 4, 61077, м. Харків, Україна
Запропоновано аналітичну модель двовимірного магнітного поля токамаків для моделювання методом тестових частинок. Показано, як шляхом зміни модельних параметрів отримати переріз плазми з різним значенням еліптичності та трикутності. Проаналізовано питання прямих втрат частинок у токамаках. Побудовано конуси втрат частинок для різних початкових радіальних положень. Для різних сортів іонів плазми числовими методами знайдено мінімальну енергію, при якій можлива пряма втрата захоплених частинок з плазми.
КЛЮЧОВІ СЛОВА: кут обертального перетворення, відображення Пуанкаре, захоплені та пролітні частинки, прямі втрати, конус втрат.

The test particle simulations play an important role in the understanding of the processes of particle transport in the present-day fusion devices such as tokamaks and stellarators. This method allows not only to verify the properties of the particle motion in the given magnetic field configuration [1] but also to estimate the radial dependence of the transport coefficients [2,3] as well as to calculate the heat loads on the different plasma-facing components [4].

Another important application of this technique is the study of different mechanisms of particle losses. In this paper we perform the numerical calculation of the particle orbits and direct losses of the hydrogen ions in a tokamak geometry. It is an important problem with respect to the fact of energetic tail production under the ICRF plasma heating in minority heating regime [5] which could decrease the plasma confinement. The purpose of the work is the study of the particle energies required to escape from the plasma for the different radial particle locations.

TOKAMAK MAGNETIC FIELD MODEL

In present-day tokamaks and stellarators the plasma is confined using the strong toroidal magnetic field. In order to compensate the radial drift and provide the confinement of particles the magnetic field should be made twisted. In stellarators the confining magnetic field is fully produced by the 3D external magnetic coils. In tokamaks the set of planar toroidal field (TF) coils is used to create the toroidal magnetic field. The rotational transform is produced due to the induced current flowing in the plasma.

In contrast to the inherent 3D structure of the magnetic field in stellarators the tokamak geometry usually has the symmetry over the toroidal direction. Neglecting the effects with the toroidal ripple of the magnetic field due to the finite number of TF coils (for example, the number of TF coils for tokamak JET is 32 but could be switched to 16 to study the enhanced ripple losses [6]) the tokamak magnetic field can be considered as a 2D structure.

We use the orthogonal curvilinear quasitoroidal coordinate system (r, θ, ϕ), where r is the radial distance from the plasma center, θ and ϕ are the poloidal and toroidal angles, respectively (Fig. 1). This coordinates are linked to the cylindrical $(R, \tilde{\phi}, Z)$ via the relations: $R = R_0 + r\cos\theta$, $\tilde{\phi} = -\phi$, $Z = r\sin\theta$, where R_0 is the major plasma radius. The Lame coefficients for the coordinate system considered are the following: $h_r = 1$, $h_\theta = r$, $h_\phi = R$. We also introduce the quantity $h(r,\theta) = h_\phi/R_0 = 1 + (r/R_0)\,\cos\theta$ which will be useful for further calculations.

The stationary equilibrium magnetic field $\vec{B}(r,\theta) = (B_r; B_\theta; B_\phi)$ should satisfy the equations:

$$\mathrm{div}\vec{B} = 0, \tag{1}$$

$$\mathrm{rot}\vec{B} = \frac{4\pi}{c}\vec{j}. \tag{2}$$

In the low β case only the toroidal component of the plasma current is non-zero. Assuming the symmetry over the toroidal direction and using the explicit expression for

$$(\mathrm{rot}\vec{B})_r = \frac{1}{r\,h}\frac{\partial}{\partial\theta}(hB_\phi) - \frac{1}{R}\frac{\partial B_\theta}{\partial\phi} = 0 \tag{3}$$

the standard radial dependence of the toroidal component of the magnetic field is obtained

$$B_\phi(r,\theta) = B_0R_0/R = B_0/h(r,\theta), \tag{4}$$

where B_0 is the magnetic field at the plasma axis.

Now we examine the expression for the divergence of the magnetic field

$$\mathrm{div}\vec{B} = \frac{1}{rR}\left(\frac{\partial}{\partial r}(rRB_r) + \frac{\partial}{\partial\theta}(RB_\theta) + r\,\frac{\partial B_\phi}{\partial\phi}\right) = 0. \tag{5}$$

Under the assumptions made it is simplified to the condition

$$\frac{\partial}{\partial r}\,(rh(r,\theta)b_r) + \frac{\partial}{\partial\theta}\,(h(r,\theta)b_\theta) = 0. \tag{6}$$

We now introduce two scalar functions Φ_1 and Φ_2 in the following way:

$$\begin{aligned} b_r(r,\theta) &= \frac{1}{r\,h(r,\theta)}\,\Phi_1(r,\theta), \\ b_\theta(r,\theta) &= \frac{1}{h(r,\theta)}\,\Phi_2(r,\theta). \end{aligned} \tag{7}$$

Then the equation (6) transforms to the condition:

$$\frac{\partial\Phi_1}{\partial r} + \frac{\partial\Phi_2}{\partial\theta} = 0. \tag{8}$$

The magnetic field $\vec{B}$ is expressed in terms of the scalar functions as follows:

$$\vec{B} = \frac{B_0}{h(r,\theta)}\begin{pmatrix} \frac{1}{r}\,\Phi_1(r,\theta) \\ \Phi_2(r,\theta) \\ 1 \end{pmatrix}. \tag{9}$$

FACTORIZATION OF THE SOLUTION

Among all the functions Φ_1 and Φ_2 which satisfy the equation (8) we will consider only the solutions that could be written in the factorized form:

$$\begin{aligned} \Phi_1(r,\theta) &= F_1(r)\,G_1(\theta) + f_1(\theta), \\ \Phi_2(r,\theta) &= F_2(r)\,G_2(\theta) + f_2(r). \end{aligned} \tag{10}$$

Using the separation of the variables one readily obtains

$$\gamma = \frac{F_1'}{F_2} = -\frac{G_2'}{G_1}, \tag{11}$$

where $F_1' = dF_1/dr$, $G_2' = dG_2/d\theta$. Due to the finiteness of the solution at $r = 0$ we have the additional condition $f_1(\theta) = 0$. Then the magnetic field model (9) transforms to the expression

$$\vec{B} = \frac{B_0}{h(r,\theta)}\begin{pmatrix} \frac{\gamma}{r}\,G_1(\theta)\,\int_0^r F_2(r')dr' \\ f_2(r) - \gamma\,F_2(r)\,\int_0^\theta G_1(\theta')d\theta' \\ 1 \end{pmatrix}. \tag{12}$$

It should be emphasized that specifying any functions $G_1(\theta)$, $F_2(r)$, $f_2(r)$ and constant γ the magnetic field model in the form (12) automatically satisfies the equations (1) and (2).

CIRCULAR MAGNETIC SURFACES CASE

If we set $\gamma = 0$ the magnetic field will have zero radial component $B_r = 0$. From the equation of the magnetic field lines

$$d\vec{r}\times\vec{B} = 0 \tag{13}$$

it is immediately obtained that the magnetic surfaces will have the circular form, r=const.

We will now connect the function $f_2(r)$ with the rotational transform profile $\iota(r)$. From (13) we obtain the equation which characterizes the twisting of the magnetic field line

$$\frac{d\theta}{d\phi} = \frac{R_0}{r}\, h(r,\theta)\, f_2(r). \tag{14}$$

Let us denote $\iota^\star(r) = (R_0/r)\, f_2(r)$. Then the magnetic field is written in such a simple form:

$$\vec{B} = B_0/h(r,\theta)\, (\vec{e}_\phi + (r/R_0)\, \iota^\star(r)\, \vec{e}_\theta). \tag{15}$$

The function $\iota^\star(r)$ is often called to be the rotational transform when using the magnetic field in a form (15). We will show below that in a general case it is not true, and $\iota^\star(r)$ is the rotational transform profile only in the limit of the large aspect ratio.

The solution of equation (14) with the initial conditions $\theta_0 = 0$, $\phi_0 = 0$ can be written in the following form:

$$\phi(\theta) = \frac{1}{\iota^\star(r)} \int_0^\theta \frac{d\theta'}{1 + (r/R_0)\, \cos\theta'}. \tag{16}$$

The principle branch of the solution valid for $-\pi < \phi < \pi$ can be found analytically

$$\phi(\theta) = \frac{1}{\iota^\star(r)} \frac{2}{\sqrt{1-(r/R_0)^2}} \operatorname{arctg}\left(\sqrt{\frac{1-r/R_0}{1+r/R_0}}\, \operatorname{tg}\left(\frac{\theta}{2}\right)\right). \tag{17}$$

For $\theta_{1,2} = \pm\pi$ we have $\phi_{1,2} = \pm\dfrac{\pi}{\iota^\star\sqrt{1-(r/R_0)^2}}$. Adopting the definition of the rotational transform we obtain

$$\iota(r) =< \Delta\theta/\Delta\phi >= \frac{\text{number of poloidal windings}}{\text{number of toroidal windings}} = \iota^\star(r)\, \sqrt{(1-(r/R_0)^2} \tag{18}$$

Here $\iota(r)$ is the exact rotational transform profile which is confirmed by the numerical integration of the field line equations. Finally, the more accurate expression for the magnetic field model with the circular magnetic surfaces and $\iota(r)$ as the rotational transform profile has the form

$$\vec{B}(r,\theta) = \frac{B_0}{h(r,\theta)} \left(\vec{e}_\phi + \frac{\iota(r)(r/R_0)}{\sqrt{1-(r/R_0)^2}}\, \vec{e}_\theta\right). \tag{19}$$

To feel the difference between two models (15) and (19), let us to use the typical parameters of the JET tokamak: $R_0 = 296\,\text{cm}$, $a = 90\,\text{cm}$, $\iota(r) = 1/(1.1 + 3.0(r/a)^2)$. The radial difference between the surfaces where $\iota(r) = 1/4$ and $\iota^\star(r) = 1/4$ is about 3 cm which could become important when the magnetic islands are presented in the plasma.

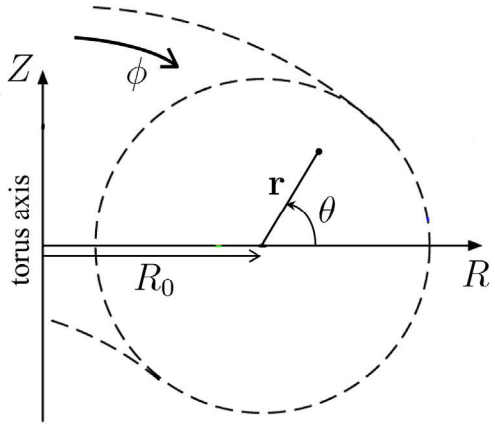

Fig. 1. The quasitoroidal coordinate system (r, θ, ϕ)

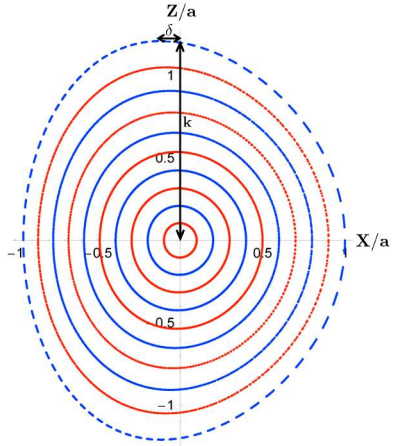

Fig. 2. Poincare plot of the D-shaped plasma surfaces

D-SHAPED MAGNETIC SURFACES

Previously the strong plasma-wall interaction was prevented by using the limiters. In the such tokamaks the magnetic surfaces have almost circular form. But now with the development of divertor concept only a few tokamaks use the limiters. Most of present-day tokamaks operate with the non-circular plasma shapes. In this section we will show how to define the model parameters to obtain the magnetic surfaces with a different ellipticity and triangularity.

The numerical integration of the magnetic field line equations

$$\begin{aligned} \frac{dr}{d\phi} &= \frac{R_0}{r}\, h(r,\theta)\, \Phi_1(r,\theta), \\ \frac{d\theta}{d\phi} &= \frac{R_0}{r}\, h(r,\theta)\, \Phi_2(r,\theta) \end{aligned} \tag{20}$$

is performed by the sixth order Runge-Kutta scheme (RK6). The initial point of each line is chosen $\theta_0 = \phi_0 = 0$. The initial radial grid is uniform, $r_{0i}/a = 0.1i$, $i = 1, 2, .., 10$. Each magnetic field line is followed for 2000 toroidal revolutions. The Poincare plot (the collection of intersection points of the magnetic field line with the chosen poloidal

plane after each toroidal turn) for the surface is produced. Except the rational magnetic surfaces where $\iota(r)$ is the ratio of two integer numbers, the magnetic field line in tokamaks is not the closed curve but fills up ergodically some surface which is called as the magnetic surface.

The elliptic surfaces are obtained if we choose $G_1(\theta) = \sin(2\theta)$. For example, defining $\gamma = 0.025$, $F_2(r) = r$, the ellipticity of the magnetic surfaces is equal to $k = 1.05$ near the axis and $k = 1.27$ at the plasma edge.

The more general form of plasma surfaces is the D-shaped configuratuion with the non-zero triangularity δ. Such surfaces can be obtained by adding the term proportional to $\sin(3\theta)$ to $G_1(\theta)$. For example, if we choose $G_1(\theta) = \sin(2\theta) - 0.5\,\sin(3\theta)$ the magnetic surfaces will have the shape shown in Fig. 2. In the considered case the ellipticity varies from $k = 1.04$ at the center to $k = 1.21$ at the edge. The triangularity increases from zero at the center to $\delta = 0.135$ at the plasma edge. The radial dependence of $k(r)$ and $\delta(r)$ could be controlled by the appropriate choice of the function $F_2(r)$.

SIMULATION RESULTS

There are two groups of particles with the different type of orbits in a tokamak. Depending on the initial particle pitch-angle $\lambda = v_{||}/v$ and the spatial location it could be either passing or trapped. The passing particles with the substantial parallel velocity rotate around the torus and form the drift surface. This surface is close to the magnetic surface but is somewhat radially shifted inward or outward depending on the sign of λ. Also the drift rotational transform which characterizes the twisting of the particle orbit differs from that of the magnetic field line. The trapped particles have low parallel velocity, at some point they are reflected from the high magnetic field side of tokamak. These particles do not complete the full turn around the torus, the poloidal projection of their orbits resembles the bananas. The banana trajectories of the hydrogen ions with the energy $W = 30\,keV$ are shown in Fig. 3. It should be noted that the trapped particles with $\lambda > 0$ turn up radially inward while the particles with $\lambda < 0$ have the outward radial motion. With the increase of the energy higher than some critical energy W_{cr} the banana width will be enough large for the particles to be lost from the plasma volume. In contrast to ripple losses or heating induced losses this mechanism of particle losses is always presented in tokamaks. It is usually called as the direct or first-orbit losses mechanism.

The separation between the trapped and passing particles in the velocity space occurs for some value of the pitch-angle λ^{crit}. In the limit of zero banana width it is given by the expression [7]

$$\lambda^{(0)} = \pm\sqrt{2\epsilon/(1+\epsilon)}, \tag{21}$$

where $\epsilon = r/R_0$ is the inverse aspect ratio of the magnetic surface considered. The result (21) stands for the case of particle location at the equatorial plane ($\theta_0 = 0$). For finite particle energies the values of λ^{crit} are slightly modified and the separation cone in velocity space becomes asymmetric.

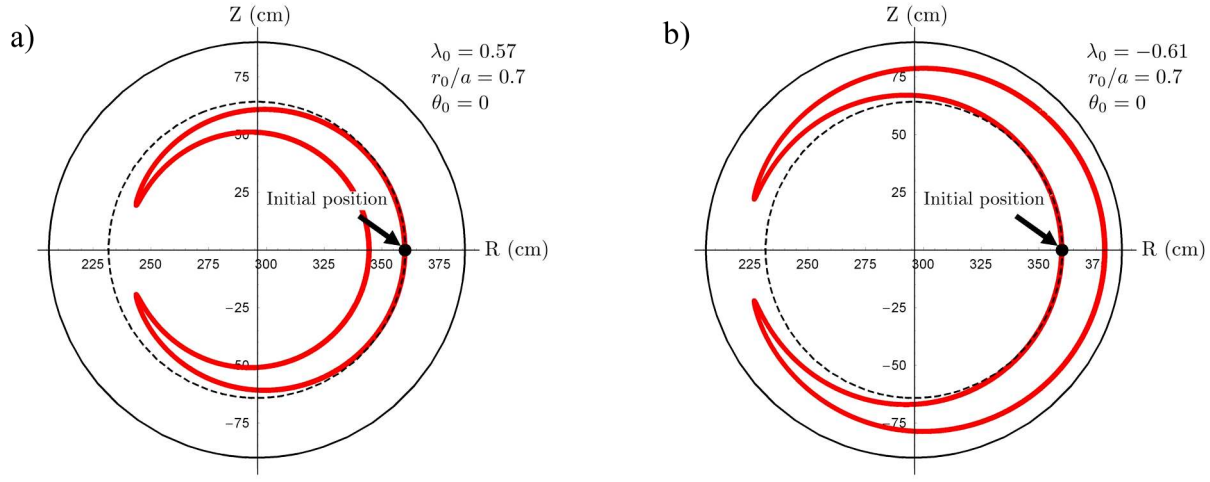

Fig. 3. The banana trajectories of the trapped particles of the hydrogen with the energy $W = 30\,keV$:
a) Inward banana trajectory $(\lambda_0 > 0)$ b) Outward banana trajectory $(\lambda_0 < 0)$

The loss cones for the hydrogen ions for two radial surfaces are shown in Fig. 4 and Fig. 5. The minimum energy W_{cr} required for the trapped particle to escape from the plasma volume for different radial magnetic surfaces has been calculated for three ion species: hydrogen, deuterium and fully ionized carbon ions. The results are presented in Table 1. As expected, the critical energy strongly decreases with the approach of initial surface to the edge. This happens due to the radical dependence of the banana width on the particle energy [8]

$$\Delta r = 2\sqrt{2}\sqrt{\frac{R_0}{r_0}}\frac{\rho_L}{\iota}, \tag{22}$$

where ρ_L is the Larmor radius and r_0 is the initial radial coordinate of the particle.

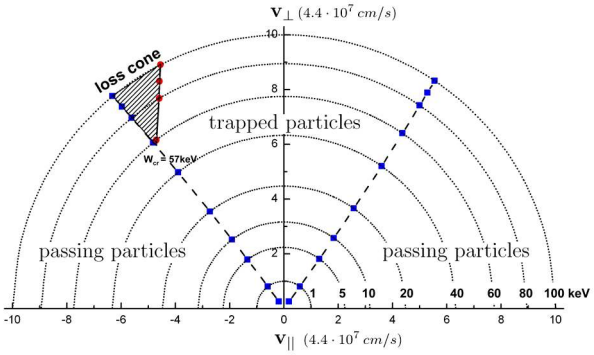

Fig. 4. Loss cone for $r_0/a = 0.7$ for hydrogen ions

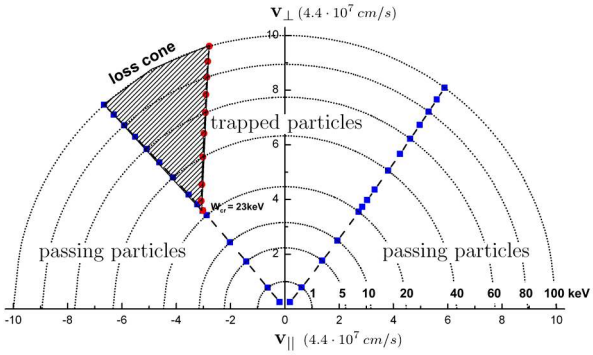

Fig. 5. Loss cone for $r_0/a = 0.8$ for hydrogen ions

Among the considered species the deuterium has the lowest critical energy. It is twice smaller than the corresponding energy for the hydrogen. It means that with the increase of atomic mass number the energy W_{cr} decreases. The carbon ions have the same charge-to-mass ratio as deuterium ions. Their critical energy is three times larger than deuterium ones. This results in the following scaling for the critical energy as a function of ion charge state number (Z) and atomic mass (A) (Table 2):

$$W_{cr} \propto Z^2/A, \tag{23}$$

which is in agreement with the results of formula (22).

Table 1. W_{cr} values for different radial locations and ion species

r_0	$\lambda^{(0)}$	λ_{crit}	Hydrogen, $A/Z=1$	Deuterium, $A/Z=2$	Carbon C^{6+}, $A/Z=2$
			$W_{cr}\,(keV)$	$W_{cr}\,(keV)$	$W_{cr}\,(keV)$
0.6	-0.556	-0.596	112	56	335
0.7	-0.592	-0.621	57	28.5	171
0.8	-0.626	-0.644	23	11.4	68.5
0.9	-0.656	-0.664	5.2	2.6	15.5

Table 2. The ratio of W_{cr} to $W_{cr,H}$ for different ion species

	H	D	T	^3He	^4He	C^{6+}	Ar^{16+}	Ar^{17+}	Ar^{18+}
$W_{cr}/W_{cr,H}$	1	1/2	1/3	4/3	1	3	6.4	7.2	8.1

The obtained dependency implies that the tritium ions have the lowest critical energy and they will be lost stronger than the rest of the ions. The impurity ions have much higher critical energy than the hydrogen isotopes. It means the impurity should be heated selectively in order to extract them without the loss of plasma confinement.

CONCLUSIONS

The analytical model of 2D tokamak magnetic field has been developed which allows the simulations of particle motion in plasma with the non-circular shape. The first orbit losses of particles have been simulated. The radial dependence of the minimal energy required for the particle to be lost from the confinement volume has been calculated. The obtained loss cones in the velocity phase space can be used to estimate the particle flux induced by the external heating.

REFERENCES

1. D.V. Sivukhin Motion of charged particles in electromagnetic fields in the drift approximation // Reviews of Plasma Physics, edited by M.A. Leontovich (Consultants Bureau, New York, 1965), Vol. 1, p. 1.
2. A.H. Boozer and G. Kuo-Petravic Monte Carlo evaluation of transport coefficients // Physics of Fluids. – 1981. – Vol. 24, №5. – P.851-859.
3. Zh.S. Kononenko and A.A. Shishkin Impurity ion dynamics near magnetic islands in the drift optimized stellarator configuration of the Wendelstein 7-X // Ukrainian Journal of Physics. – 2008. – Vol.53, №5. – P.438-442.
4. E. Strumberger Deposition patterns of fast ions on plasma facing components in W7-X // Nuclear Fusion. – 2000. – Vol. 40, № 10. – P.1697-1713.
5. M.-L. Mayoral et al Hydrogen plasmas with ICRF inverted minority and mode conversion heating regimes in the JET tokamak // Nuclear Fusion. – 2006. –Vol. 46, № 7. – P.S550-S563.
6. P.C. de Vries et al Effect of toroidal field ripple on plasma rotation in JET // Nuclear Fusion. – 2008. – Vol.48, №3. – P.035007-035012.
7. J. Wesson Tokamaks. - Oxford, U.K.: Clarendon Press, 3rd edition, 2004. – 749 p.
8. E.D. Volkov, V.A. Suprunenko and A.A. Shishkin Stellarator. – Kiev: Naukova dumka, 1983 – 310 p. (in Russian)